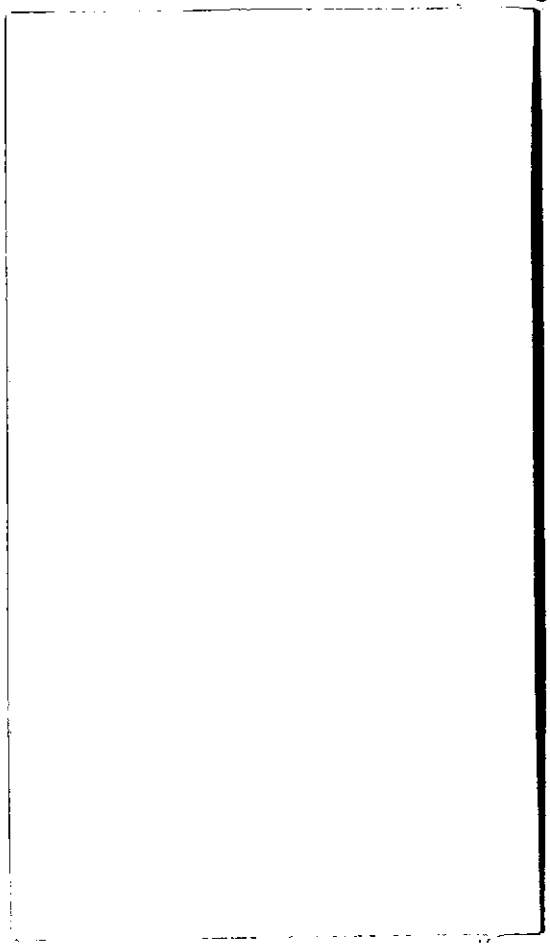

Department of
ELECTRICAL ENGINEERING
UNIVERSITY OF NOTRE DAME, NOTRE DAME, INDIANA

NASA CONTRACTOR REPORT

NASA CR-132348

Electrode Materials for Charge Coupled Devices

by W. J. Gajda, Jr.

October 1973

ELECTRODE MATERIALS FOR CHARGE COUPLED DEVICES

W. J. Gajda, Jr.

October 1973

Prepared under Contract No. NAS 1-12468 by
University of Notre Dame du lac
Notre Dame, Indiana

Langley Research Center
NATIONAL AERONAUTICS AND SPACE ADMINISTRATION

FOREWARD

The final report was prepared by the University of Notre Dame du lac, Notre Dame, Indiana for NASA's Langley Research Center under NASA Contract No. NAS 1-12468. It describes work performed from June 3, 1973 to October 16, 1973 in the Electrical Engineering Department. The Project Scientist is Dr. W. J. Gajda, Jr.

The integrated circuit processing was carried out by Dr. Gajda using the facilities of the Microelectronics Section, Telecommunication Research Branch, Flight Instrumentation Division, Langley Research Center.

The subsequent electrical and optical testing was performed using the facilities of the Electrical Engineering Department.

I. INTRODUCTION

Charge coupled semiconductor devices (CCDs) are presently under development as solid state imaging arrays. In such applications, the minority carriers created by the incident light field are stored as charge packets under suitable electrodes from which the packets are sequentially shifted (by changing the potentials of the electrodes) out of the array for subsequent processing, transmission and eventual display.

The electrode material must satisfy two primary requirements: it must be as transparent as possible (so as to allow the creation of a maximum number of carriers by a given light level) and must have as low a sheet resistivity as possible (so as to reduce the RC time constant of the electrode structure and thus allow operation of as high a frequency as possible).

Polycrystalline silicon (often shortened to poly or polysilicon in the following) has been used for electrode realization and the work described herein was carried out as part of an effort to more fully characterize the optical and electrical properties of this material.

II. TEST DEVICE DESIGN

Several approaches can be envisioned to the problem of measuring the optical transmission of polysilicon. To examine some of these options, consider the structure shown in Figure 1

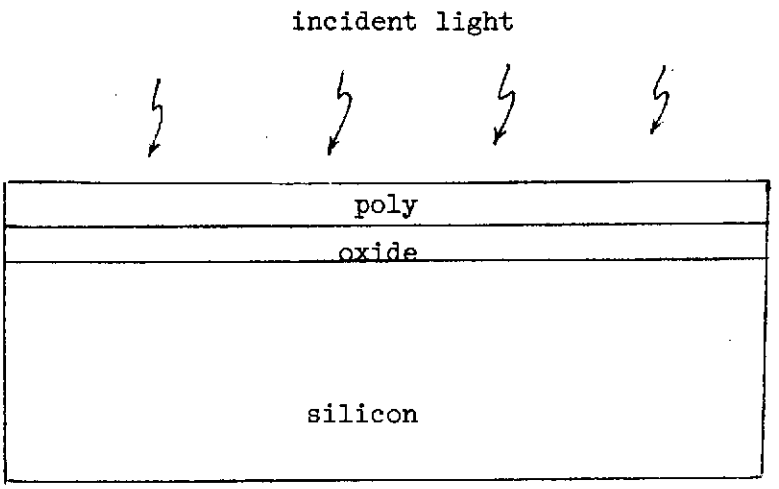

FIGURE I

This illustrates the essential planar structure which exists in the optically active regions of CCD imaging arrays. What is important is not the optical properties of the poly but rather the number of carriers which are optically generated in the silicon substrate. A realization of this properly focuses attention on the entire three layer structure (poly-silicon dioxide-silicon). It is this 'sandwich' for which optical data is desired. With this insight, schemes involving the physical 'floating' of the poly by chemical etching of the SiO_2 layer can be disregarded. Even if successful, they will not yield the desired information.

It was then decided to fabricate both photoresistors and photodiodes according to the simplified schematics of Figure 2.

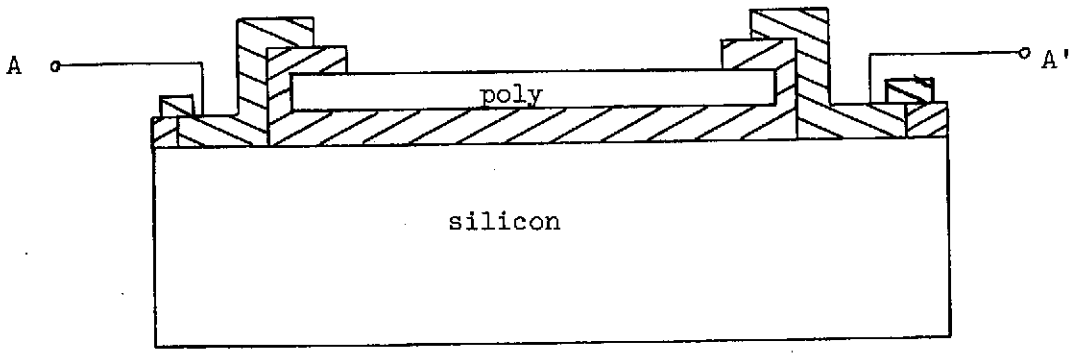

Photoresistor

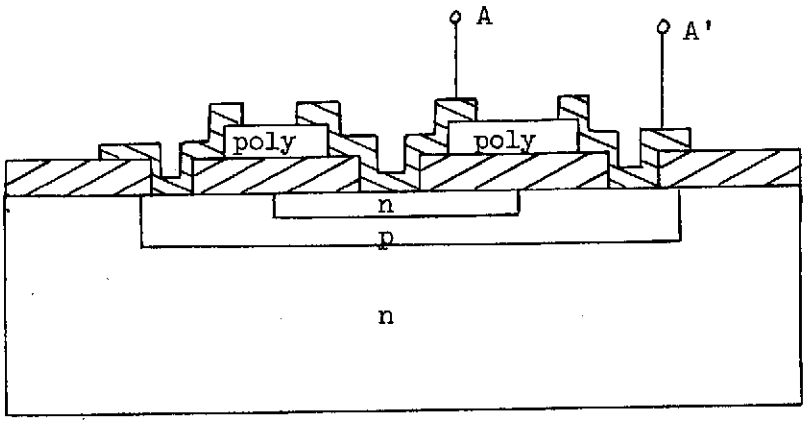

Photodiode

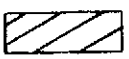

oxide

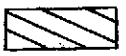

aluminum

Figure 2

For the photoresistor, the incident light will create carriers in the silicon substrate thereby modulating the resistance measured between the terminals. This change in resistance, from unilluminated to illuminated, can be related (as will be demonstrated) to the optical transmission of the poly-SiO_2-Si structure.

The set of processing steps used in fabricating the photoresistor samples is as follows.

1) clean the silicon substrate,
2) thermally oxidize,
3) grow the poly layer,
4) thermally oxidize the poly,
5) apply photoresist, expose to mask PM1 (Figure 3),
6) etch exposed oxide,
7) etch exposed poly,
8) reclean,
9) reoxidize,
10) apply photoresist, expose to mask PM2 (Figure 4),
11) etch exposed oxide,
12) reclean,
13) evaporate aluminum contacting layer,
14) apply photoresist, expose to mask PM3 (Figure 5),
15) etch exposed aluminum,
16) reclean,
17) sinter samples to provide ohmic contact.

Edge views of the samples are shown in Figure 6 at various processing points.

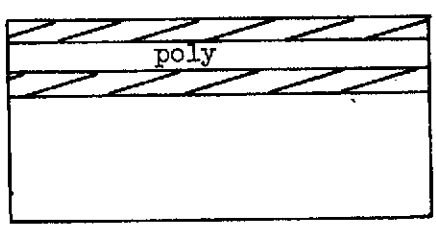

Step 6

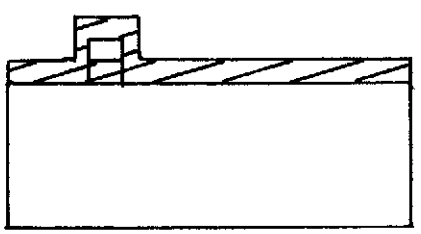

Step 11

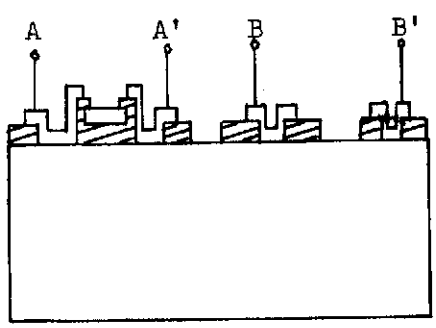

Step 19

Figure 6

Figure 3

Mask PM1 (100X)

L - light, D - dark

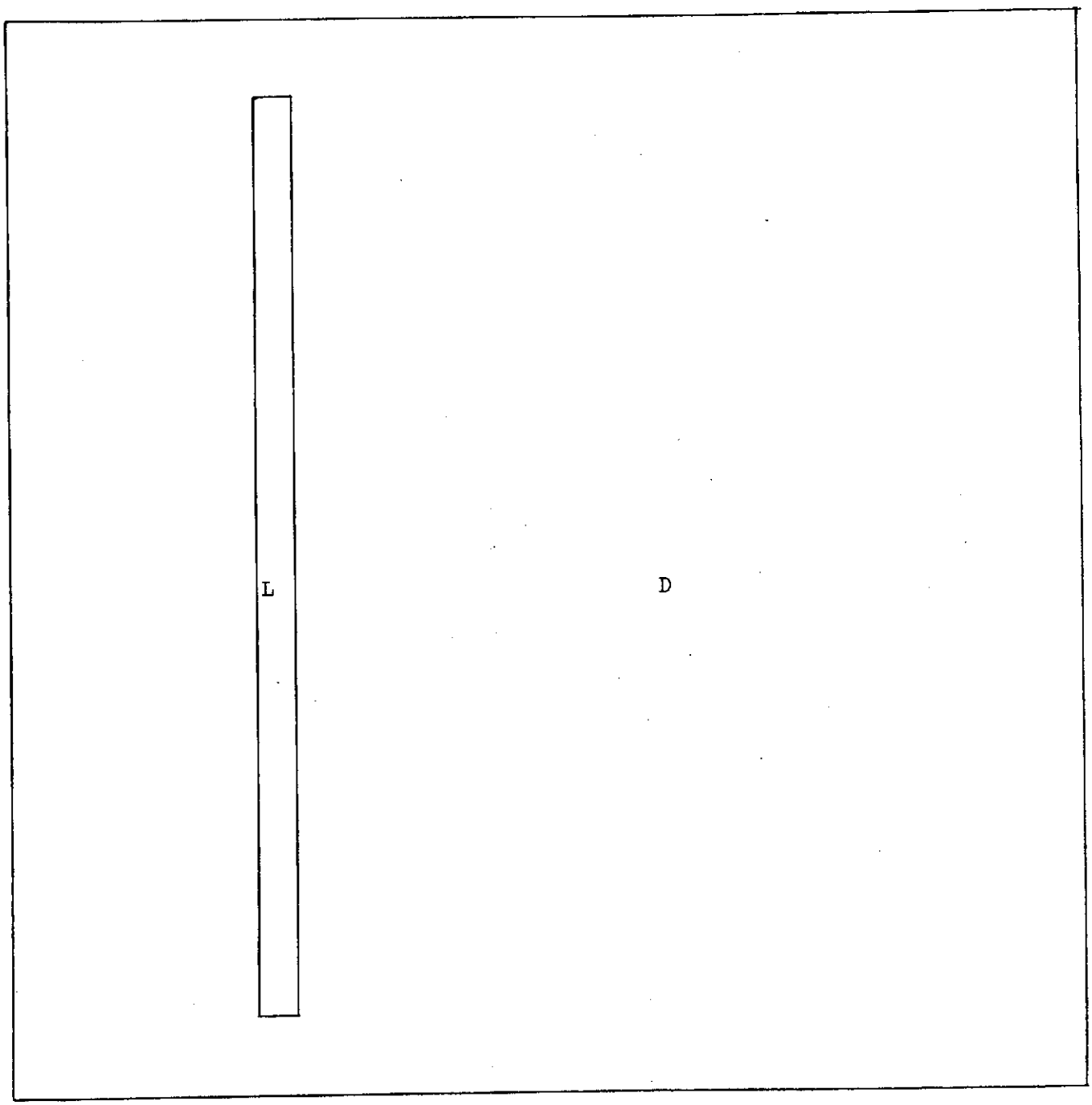

Figure 4

Mask PM2 (100X)

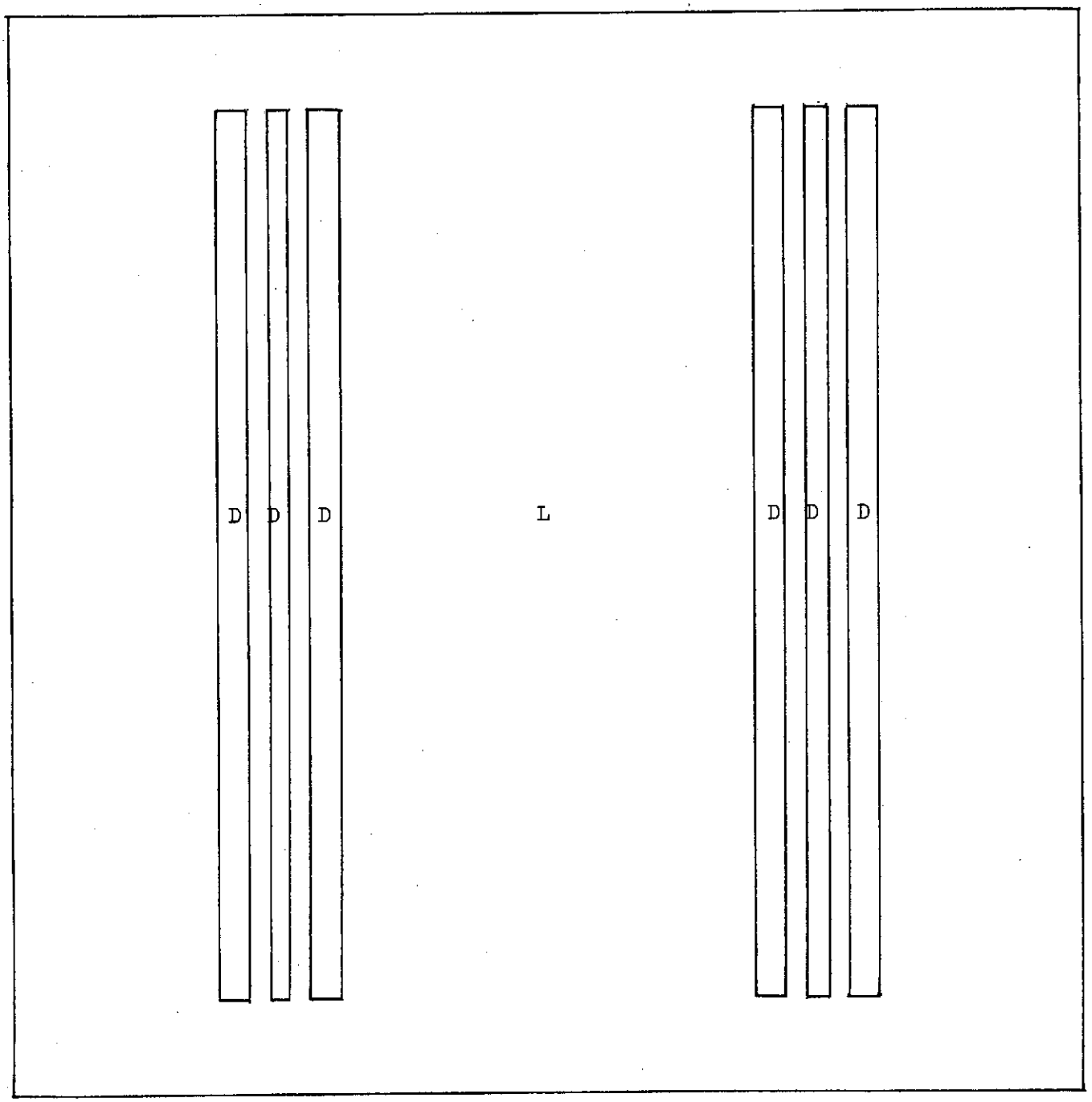

Figure 5

Mask PM3 (100X)

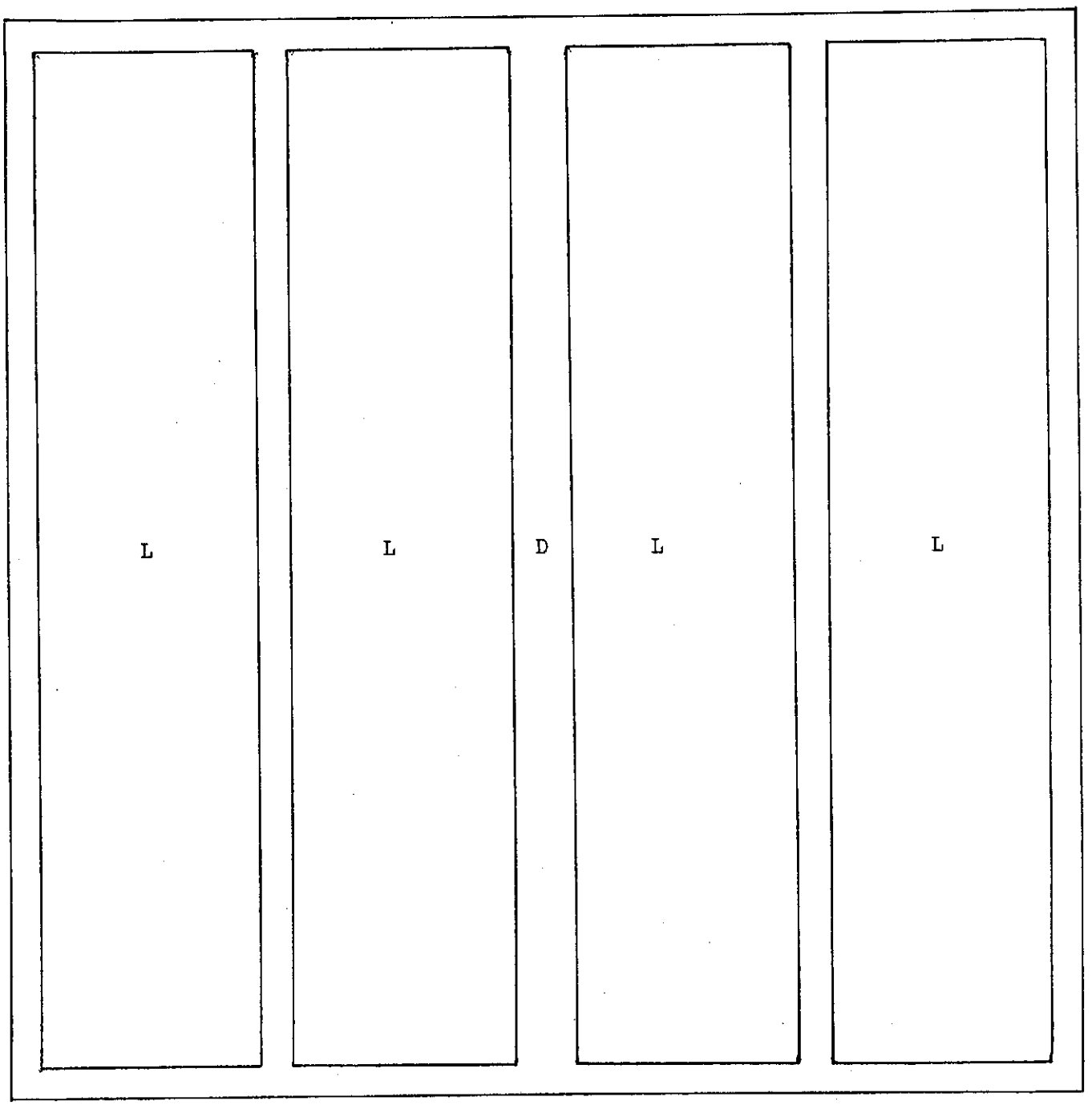

Two pairs of contacts are provided on each wafer and the photoconductance measured across the terminal pair A-A' is related to the amount of light that penetrates to the substrate. The terminals B-B' are provided as a control comparison since the surface of the silicon is bare between this pair.

After fabrication, the wafers were sawn apart along the center line to physically separate the two elements.

Since the effect sought is photoconductance modulation, the highest resistivity substrates available were used. The starting silicon was 30-50 ohm-cm, (111) oriented and p type. The formation of ohmic contacts without the necessity of an n^+ diffusion was made possible by the choice of a p type substrate.

A total of forty samples of this kind were fabricated and the essential values of the processing parameters are given in table I.

These samples were tested and displayed an easily measurable photoconductance but the change from sample to sample was small and it was anticipated that a synchronous measurement scheme (a mechanically chopped incident beam and a lock-in amplifier detector) would be needed to observe the effects of poly film thickness and doping changes.

Rather than pursue this, it was decided to fabricate a set of more optically sensitive samples by using a diode geometry. For these structures, the incident light will create carriers in the silicon substrate thereby modulating the reverse saturation current of the diodes. This change in saturation current can be related (as will be demonstrated) to the optical transmission of the poly-SiO_2-Si sandwich.

The set of processing steps used in fabricating the photodiodes is as follows

1) clean the silicon substrate,
2) thermally oxidize,
3) apply photoresist, expose to mask M1 (Figure 7),
4) etch exposed oxide,
5) reclean,
6) p-type diffusion,
7) apply photoresist, expose to mask M2 (Figure 8),
8) Etch exposed oxide,
9) reclean,
10) n^+ diffusion,
11) strip all oxide,
12) reclean,
13) reoxidize,
14) grow poly,
15) oxidize poly,
16) apply photoresist, expose to mask M3 (Figure 9),
17) etch exposed oxide,
18) etch exposed poly,

TABLE I

PHOTORESISTOR FABRICATION

Sample ID	polysilicon growth Temp. °C	Time min.	doping gas conc. (ppm)	thickness microns	R_s ohms	ρ ohm-cm.
B1	1035	1	.0036	.22	*	
B2	1035	1	.0036	.24	*	
B3	1035	4	.0036	2.53	*	
B4	1035	4	.0036	2.58	*	
B5	1035	1.5	.0036	.78	*	
B6	1035	2	.0036	1.07	*	
B7	1035	3	.0036	1.64	*	
B8	1025	2	none	1.1	*	
B9	1025	2	none	1.03	*	
B10	wafer damaged during processing					
B11	1025	2	.01	.98	*	
B12	1025	2	.01	1.01	*	
B13	1025	2	.0073	.86	*	
B14	1025	2	.0073	.94	*	
B15	1025	2	.0014	.93	*	
B16	1025	2	.0014	.95	*	
B17	1025	2	none	.92	*	
B18	1025	2.5	none	1.37	*	
B19	1025	3	none	1.79	*	
B20	1025	3	none	1.83	*	
B21	1025	3.5	none	2.11	*	
B22	1025	4	none	2.3	*	
B23	1050	2	.0036	1.06	*	
B24	1050	1.5	.0036	.74	*	
B25	1050	1.5	.0036	.71	*	
B26	1125	1.25	.0036	.63	*	
B27	1125	1.25	.0036	.58	*	
B28	1025	1.25	.0036	.72	*	
B29	1025	1.25	.0036	.71	*	
B30	1025	3.5	none	2.14	*	
B31	1025	4	none	2.35	*	
B32	1050	2	none	.98	*	
B33	1030	1	.014	.28	$4.3(10^7)$	1200.
B34	1030	1.25	.014	.41	$7.6(10^6)$	310.
B35	1030	1.5	.014	.73	$3.3(10^7)$	240.
B36	975	1	.014	.36	$3.3(10^7)$	1200.
B37	975	1.25	.014	.52	$1.8(10^6)$	940.
B38	975	1.5	.014	.68	$1.3(10^5)$	89.
B39	975	1	.048	.55	$2.4(10^4)$	13.2
B40	975	1.25	.048	.61	$8.5(10^4)$	5.2

Notes: the reactor silane concentration was .37% during all poly growths, diborane was used as the doping gas in all cases,

all oxidations were identical, dry nitrogen was bubbled through 194°C water, the furnace temperature was 1100°C and the resultant oxide thickness was calculated to be 5300A.

*the sheet resistance was too large to be measured on available instruments

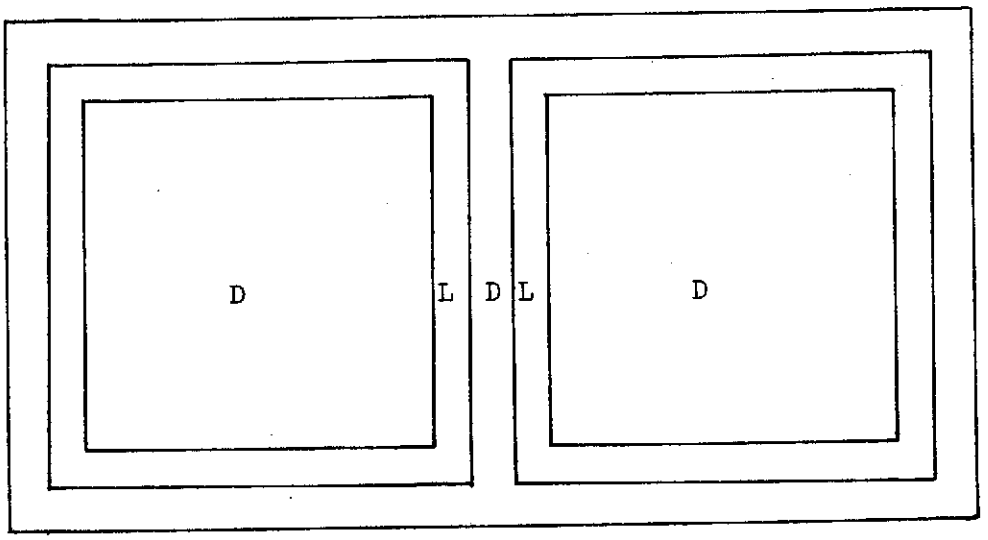

M1

Figure 7

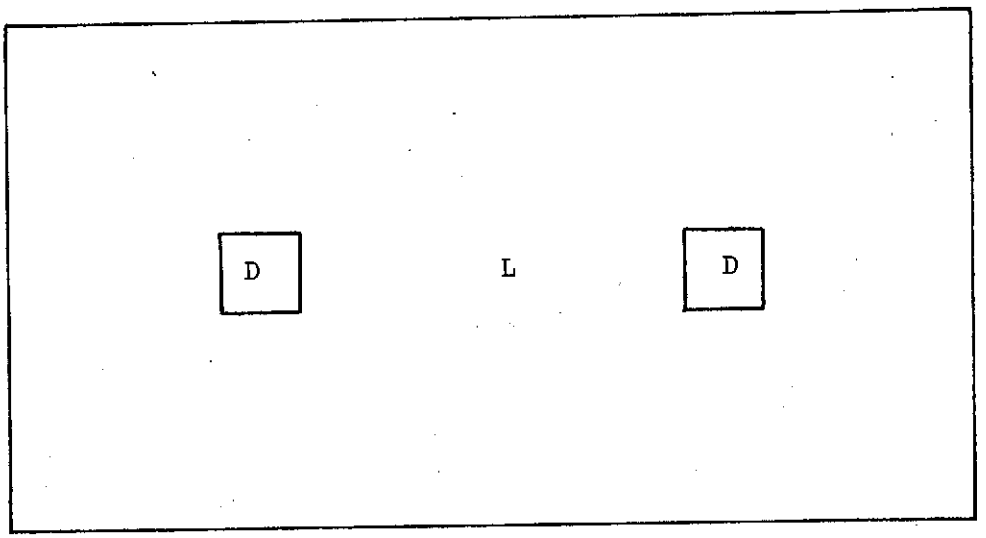

M2

Figure 8

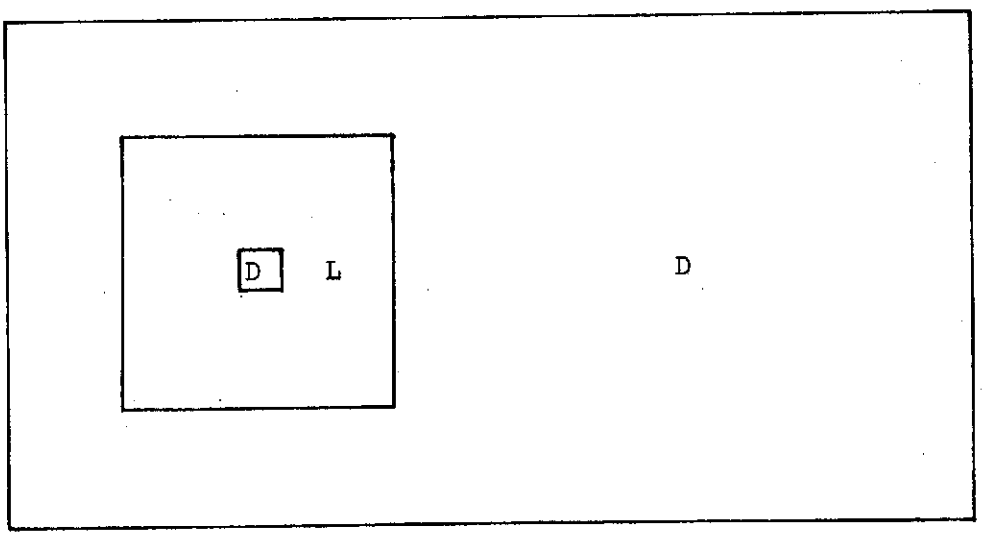

M3

Figure 9

(100X)

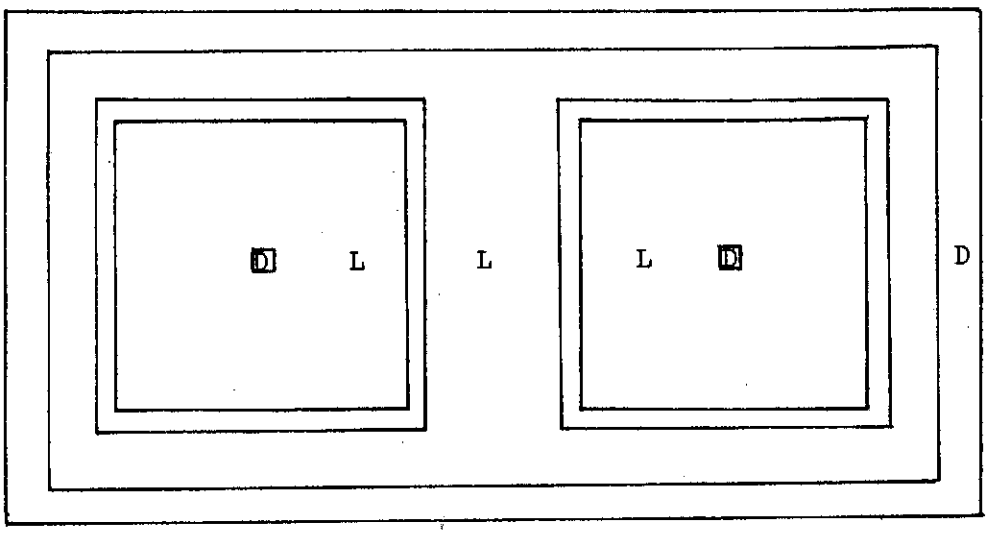

M4

Figure 10

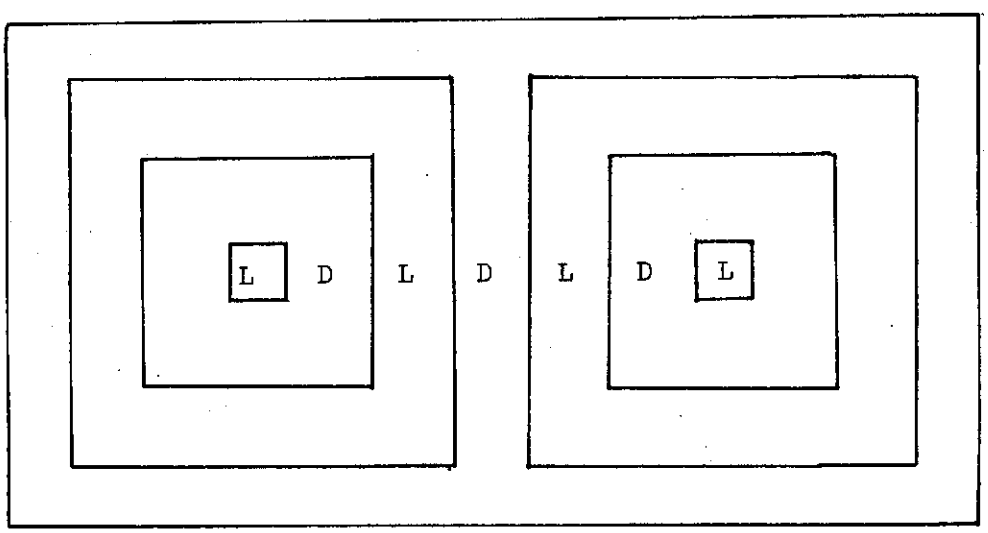

M5

Figure 11

(100X)

20) reclean,
21) reoxidize,
22) apply photoresist, expose to mask M4 (Figure 10),
23) etch exposed oxide,
24) reclean,
25) evaporate aluminum,
26) apply photoresist, exposed to mask M5 (Figure 11),
27) etch exposed aluminum,
28) reclean,
29) sinter samples to provide ohmic contact.

Edge views of the samples at various processing points are shown in Figure 12.

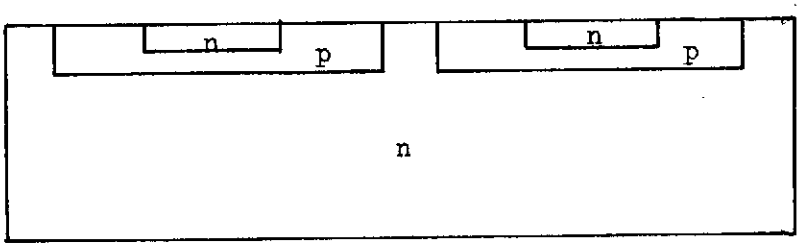

Step 12

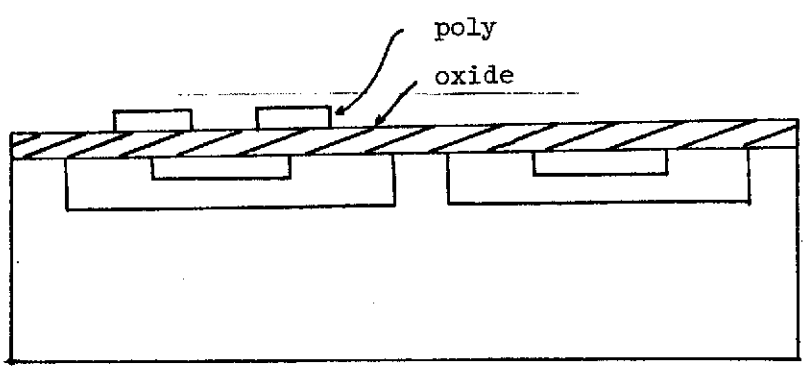

Step 19

Figure 12

As is the case of the photoresistors, two photodiodes were fabricated on each wafer - one in which the poly - SiO_2 layers the optically active regions and one in which the active region was bare.

After fabrication, the wafers were sawn apart along the center line to physically separate the two photodiodes.

The starting material was 10 Ω-cm, (111) oriented, n type silicon in all cases.

A total of forty samples of this kind were fabricated and the essential values of the processing parameters are given in Table II.

Ten samples were fabricated following this procedure with one additional processing step.

p diffusion into poly (after step 14)

This was done to reduce the sheet resistance of the as-grown poly and proved to be quite effective, as will be discussed in section IV, even for thin layers which display large as-grown sheet resistances.

These samples were tested for light sensitivity and displayed sufficient response so as to allow the desired optical and electrical testing. The details and results of these measurements are given in section IV of this report.

It should be noted that the designs of the test devices, by leaving the poly-SiO_2-Si structure in place, a-priori take into account the effects of optical interference due to the film thicknesses and the various interfaces used in construction since these layers are not disturbed prior to electrical and optical measurement.

All of the steps listed in the above two processing sequences are standard procedures used in the microelectronics facilities at Langley Research Center. The poly growths were carried out in an epitaxial reactor with silane used as the silicon source. The carrier gas was hydrogen and metered amounts of diborane or phosphine were introduced for doping. The substrate growth temperatures listed in tables I and II are uncorrected optical pyrometer readings.

TABLE II

PHOTODIODE FABRICATION

Sample ID	polysilicon growth Temp. °C	Time min.	doping gas conc. (ppm)	thickness microns	R_s ohms	ρ ohm-cm.	poly diffusion?
A1	1035	1.5	.0036	.81	*		no
A2	1035	2	.0036	1.02	*		no
A3	used as a p-type diffusion monitor						
A4	1035	3	.0036	1.48	*		no
A5-A8	photoresist overbaked and samples were destroyed						
A9-A16	poor p-type diffusion and samples were destroyed						
A17	1000	1	.137	.29	2600	.075	no
A18	1000	2	.137	.97	24	.0023	yes
A19	1000	2	.137	1.04	1230	.128	no
A20	damaged in processing						
A21	1000	4	.137	2.1	9.6	.002	yes
A22	used for diode test only, no poly growth						
A23	1000	4	.137	2.2	423	.093	no
A24-A27	used for diode test only, no poly growth						
A28	1030	1	.014	.25	187	.0047	yes
A29	1030	1.25	.014	.37	98	.0036	yes
A30	1030	1.5	.014	.72	59	.0043	yes
A31	975	1	.014	.36	168	.006	yes
A32	975	1.25	.014	.52	57	.003	yes
A33	975	1.5	.014	.61	54	.0033	yes
A34	975	1	.048	.54	179	.0097	yes
A35	975	1.25	.048	.56	92	.0092	yes
A36	975	1.5	.048	.66	52	.0034	yes
A37	975	1.5	.048	.67	61656	4.1	no
A38	975	1	.048	.52	96	.005	yes
A39	used as an n-type diffusion monitor						
A40	1000	1	.137	.27	117	.0032	yes

Notes: the reactor silane concentration was .37% during all poly growths,
diborane was used as the doping gas in all cases,
all oxidations were identical to those used in photoresistor fabrication,
poly diffusion parameters:

predeposition - 100 cc/min. of 5000 ppm diborane
1000 cc/min. nitrogen
200 cc/min. 50% nitrogen - 50% oxygen
1100°C for 10 minutes

drive - wet, gases bubbled through 194°C water,
1000 cc/min. nitrogen
200 cc/min. 50% nitrogen - 50% oxygen
1100°C for 30 minutes
- dry, same gas flows as for wet drive
1100°C for 60 minutes

* the sheet resistance was too large to be measured on available instruments.

III. DEVICE ANALYSIS

A) Photoresistors

In considering these devices, the basic optical effect is conductivity modulation due to the optical generation of carriers by the incident light. This will be a majority carrier effect except in situations involving near-intrinsic material (the majority and minority carrier concentrations being numerically nearly equal) under low level injection or high level injection (the excess carrier concentrations being much greater than the equilibrium densities.)

To develop a quantitative description of this process of photoconductivity modulation, write

$$\sigma = q\ (\mu_e n + \mu_h p)$$

$$\sigma_0 = q\ (\mu_e n_o + \mu_h p_0)$$

where σ, σ_0 are the light, dark conductivities, μ_e, μ_h the electron, hole mobilities, q the magnitude of the electron charge, n, p the electron, hole concentrations and the subscript 0 indicates equilibrium.

Defining a relative change in photoconductivity R_{pcm} as

$$R_{pcm} = \frac{\Delta\sigma}{\sigma_0} = \frac{\sigma-\sigma_0}{\sigma_0}$$

one obtains

$$R_{pcm} = \frac{\mu_e n' + \mu_h p'}{\mu_e n_0 + \mu_h p_0}$$

where n', p' are the excess electron, hole densities,

$$n' = n-n_0$$

$$p' = p-p_0$$

Defining a mobility ratio b (μ_e/μ_h) and assuming low level injection, non-degenerate material and quasi space charge neutrality,

$$R_{pcm} = \frac{(1+b)p'p_0}{p_0^2+bn_i^2}$$

where n_i is the intrinsic carrier concentration.

To find a condition on p_0 under which R_{pcm} is a maximum, set

$$\frac{dR_{pcm}}{dP_0} = 0$$

with the result

$$p_0 = \sqrt{b}\, n_i$$

A direct check of the second derivative indicates that this is indeed a condition for a maximum.

Since b is greater than one for silicon, the last equation indicates that a photoresistor will display maximum sensitivity when composed of material which is near-intrinsic p type. The material used in the photoresistor fabrication is as close to this optimum as could be readily obtained.

B) Photodiodes

Because the major objective of this program was to obtain optical data for potential charge coupled device electrode materials, no detailed analysis of the optical response of photodiodes was deemed necessary. However a simple model based on the following set of idealizations has been included.

The basic device model is shown in Figure 13. It is an abrupt junction, $N_D(cm^{-3})$ is the donor concentration on the n side, $N_A(cm^{-3})$ the acceptor concentration on the p side and the effect of light flux (intensity Φ) is to generate $K\Phi$ hole-electron pairs/cm^3-sec uniformly throughout the device

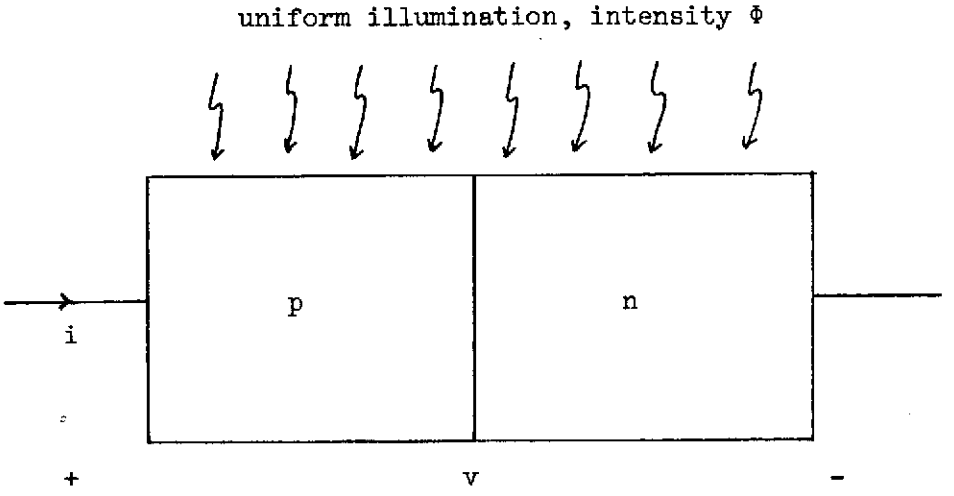

Figure 13

The following assumptions are invoked to simplify the analysis.

a) Recombination-generation is neglected in the space charge layer of the device, i.e., the hole and electron currents are constant across the space charge layer,
b) only low level injection is considered,
c) the neutral regions are much greater in length than the minority carrier diffusion lengths,
d) minority carrier drift current is negligible in the neutral regions,
e) only the D.C. steady state is analyzed and
f) both the p and n regions are extrinsic.

Under these conditions, the excess minority carrier concentrations at the edges of the space charge layer are related to the applied voltage v by the well-known[1] equations

$$p_n' = p_{n0} \left(e^{\frac{qv}{KT}} - 1\right)$$

$$n_p' = n_{p0} \left(e^{\frac{qv}{KT}} - 1\right)$$

where K is Boltzmann's constant, T the absolute temperature is degrees Kelvin and p_{n0}, n_{p0} are the equilibrium minority carrier concentrations in the neutral regions.

Using the geometry of Figure 14,

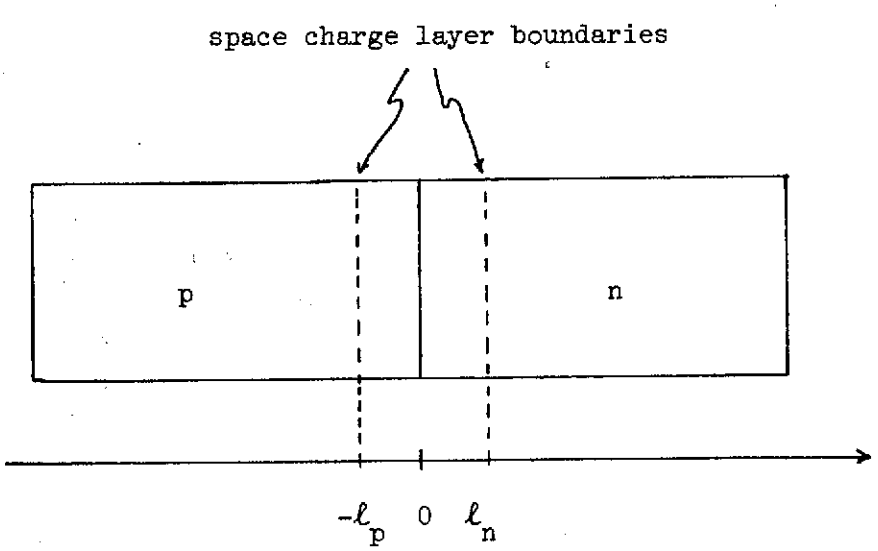

Figure 14

the excess hole concentration in the n region is found from the equation

$$D_h \frac{\delta^2 p_n'}{\delta x^2} - \frac{p_n'}{\tau_h} = - K\Phi$$

and the excess electron concentration in the p region is found from the equation

$$D_e \frac{\delta^2 n_p'}{\delta x^2} - \frac{n_p'}{\tau_e} = - K\Phi$$

Solving and using the above boundary conditions,

$$x>\ell_n,\ p_n'(x) = [p_{no}(e^{\frac{qv}{KT}} - 1) - K\Phi\ \tau_h]e^{-(\frac{x-\ell_n}{L_h})} + K\Phi\tau_h$$

$$x<-\ell_p,\ n_p'(x) = [n_{p0}(e^{\frac{qv}{KT}} - 1) - K\Phi\tau_e]e^{(\frac{x+\ell_p}{L_e})} + K\Phi\tau_e$$

In the above,

D_e, D_h are electron, hole diffusion coefficients,

τ_e, τ_h are electron, hole minority carrier lifetimes and

L_e, L_h are electron, hole diffusion lengths.

With the excess minority carrier concentrations known throughout the neutral regions, the total diode current i may be calculated. The result is

$$i = qA\ [-K\Phi(L_e+L_h)] + I_0(e^{\frac{qv}{KT}} - 1)$$

where A is the cross sectional area of the diode. It is seen that the current consists of two parts, the first due to the optical generation of carriers and the second the dark current. I_0 is the dark saturation current and is given by the expression

$$I_0 = qA[\frac{D_e}{L_e} n_{p0} + \frac{D_h}{L_h} p_{n0}]$$

The i-v characteristic is plotted in Figure 15

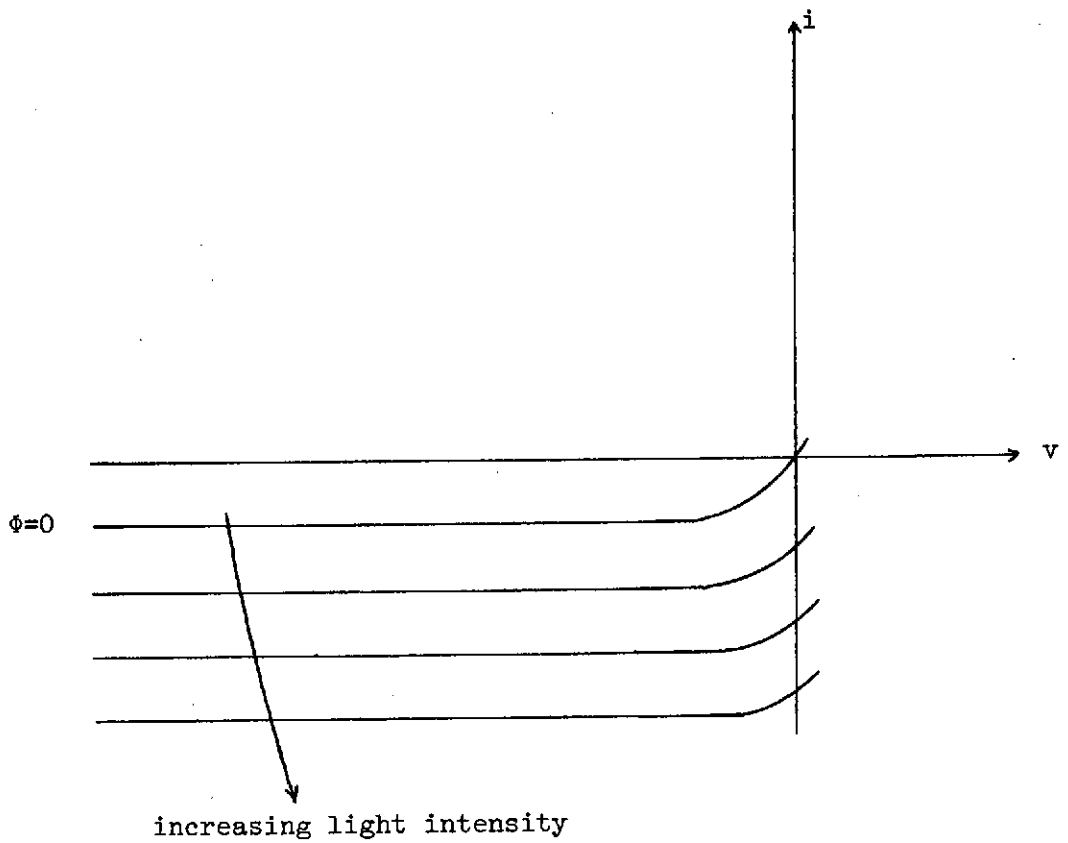

Figure 15

Defining a relative change in saturation current R_{pDm} as

$$R_{pDm} = \frac{\Delta I_0}{I_0} = \frac{I_{SAT}\ (\text{light}) - I_{SAT}(\text{dark})}{I_{SAT}(\text{dark})}$$

we obtain

$$R_{pDm} = \frac{K\Phi(L_n + L_e)}{\frac{D_h}{L_h} p_{n0} + \frac{D_e}{L_e} n_{p0}}$$

C) Comparison of the Sensitivities

Using the results from section III-A and section III-B, the sensitivity ratio

$$R_{PDM}/R_{PCM}$$

may be written

$$\frac{R_{PDM}}{R_{PCM}} = \frac{L_e + L_h}{\frac{D_e}{L_e} n_{p0} + \frac{D_h}{L_h} p_{n0}} \quad \frac{bn_i^2 + p_0^2}{(1+b)\,\tau_h p_0}$$

where $p' = K\Phi\tau_h$

It should be carefully noted that our writing of the external generation rate in the form $K\Phi$ was not necessary in arriving at this ratio. Any more general function describing the optical generation would have appeared in the expressions for both R_{PDM} and R_{PCM} (since the equations used in our derivations are all linear) and would cancel in this final ratio.

Substituting appropriate numerical values,

$$\frac{R_{PDM}}{R_{PCM}} = 10^6$$

The relative change in the photodiode current is thus seen to be much greater than the relative change in photoconductance so the experimental results mentioned in section II are not surprising.

IV. EXPERIMENTAL RESULTS

A) Optical and Electrical Properties of Polysilicon

i) Electrical Measurements

The reported values for the sheet resistance (R_s) of the polysilicon layers were obtained by four point probe measurements which were made immediately after growth and after the poly diffusion step (if any).

In all cases, the reported values of sheet resistance are average values found by a least squares fit to a plot of probe current versus probe voltage over the range of voltage, 5 to 40 volts.

The resistivity ρ (ohm-cm) of the films is related to the sheet resistance by the equation

$$\rho = R_s t$$

where t is the film thickness in cm.

ii) Thickness Measurements

The reported values of poly layer thickness were obtained using multiple beam interferometry. When the sample wafers were sawn apart, the scraps with poly overgrowth were saved and the top SiO_2 layer etched away. The exposed poly was then partially masked with apiezon wax and a stop was etched into it. Silver was evaporated over this step and the poly layer thickness was measured by observing the fringes of equal chromatic order formed by the step in contact with an optical flat. It should be noted that the reported values of thickness are determined after all processing and thus include the effects of post-growth thermal oxidation in thinning the poly layers. The reported numbers are <u>not</u> the as-grown thicknesses.

iii) Optical Measurements

The monochromatic incident light was produced by a monochrometer with an achromatic collimating lens at the output slit and an achromatic converging lens to focus the collimated beam onto the active regions of the sample. Razor blade slits were used to define the geometry of the incident light. Figure 16 shows the experimental set-up.

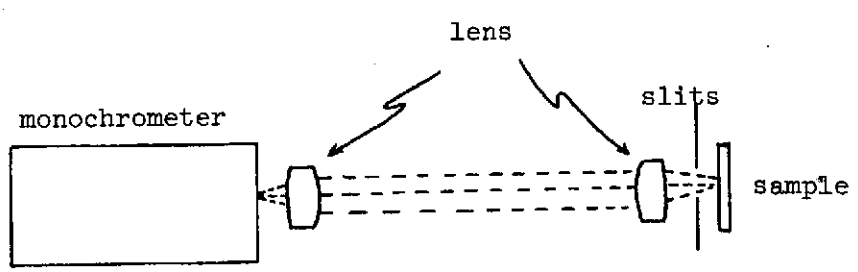

Figure 16

The method used to determine the optical absorption of the poly-SiO_2-Si sandwich was quite direct. It should be recalled that the photodiodes were fabricated in pairs-one in which the multilayer structure covered the active region of the device and one in which the active region was bare.

First the sandwichless diode was inserted into the sample holder and probes placed on the contacting pads. A reverse bias, on the order of -1 to -5 volts) was applied to the diode to insure its operation in a region of saturation current. The output of the optical system was focused onto the diode and the variation of saturation current as a function of monochromator wavelength was recorded.

Then neutral density optical filters (of known absorption) were placed into the optical path and the saturation current recorded as a function of wavelength and added absorption. A result as shown in Figure 17 was obtained.

The corresponding sandwich diode was then placed into position and the measurement repeated with no filters in the optical path. The output slit of the monochromator and the razor blade slits in front of the sample were wide enough to insure uniform illumination of the sensitive region of the diode hence positioning was not critical and the experimental results were found to be insensitive to small shifts in sample position with respect to the incident light beam.

The saturation current as a function of wavelength for the sandwich diode is not a smooth function but rather displays quasi periodic structure as a consequence of interference effects between the waves reflected from the interfaces[2,3]. This structure was removed by fitting a smooth curve as sketched in Figure 18.

By plotting this curve on the family found in Figure 17, a value for the optical absorption of the poly and SiO_2 can be found which does not include the effects of interference. Since the optical absorption of SiO_2 is Known[6] and the thickness of this layer is known from the oxidation parameters, the absorption of the poly can be found

$$\alpha_{poly} t_{poly} = (\alpha t)_{total} - (\alpha t)_{SiO_2}$$

Upon dividing this quantity by the poly thickness, the absorption coefficient as a function of wavelength becomes known.

The values of α_{poly} are shown in Table III. All measurements were made at room temperature only and covered the optical range of 4500 to 8000A in wavelength.

From the viewpoint of suitability for use as CCD imaging array electrodes, the most transparent films obtained were poly layers with final thicknesses around 2500A with absortions around 1 at 4500A wavelength, .4 at 6000A wavelength and .1 at 7500A wavelength; the sheets resistances of these films were on the order of 100 ohms and they underwent a boron diffusion after growth.

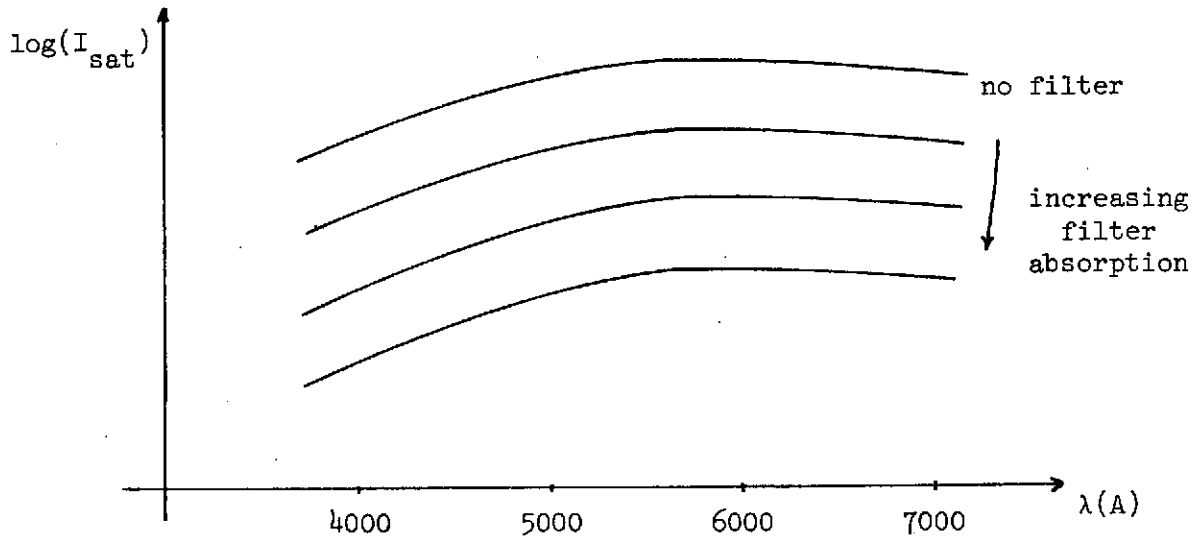

Figure 17 - bare photodiode

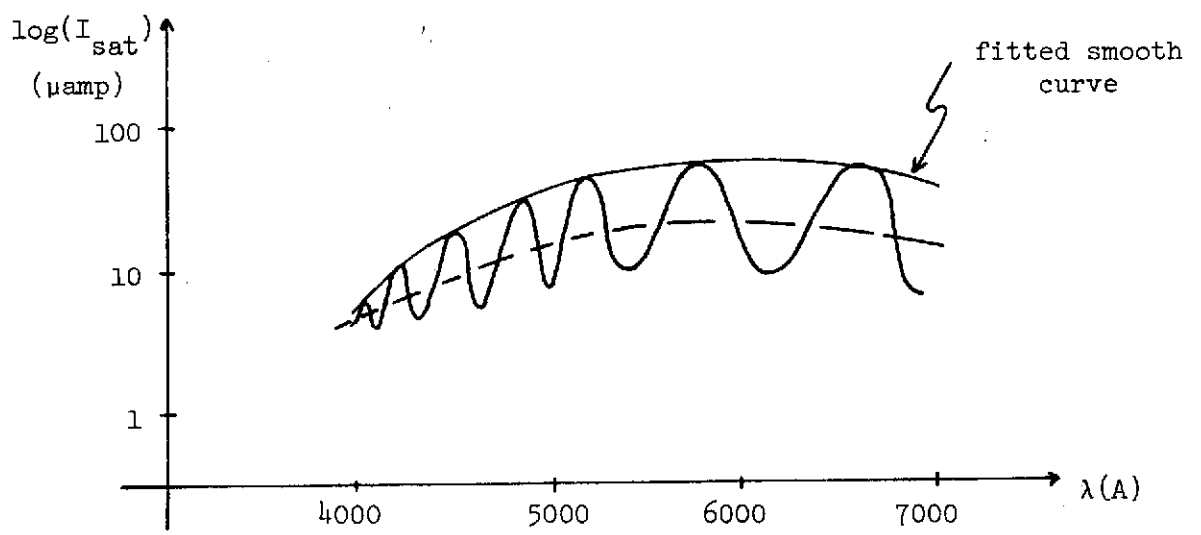

Figure 18 - photodiode covered with poly-SiO_2 sandwich

NOTE: both of these figures are plotted by hand because an automatic plotter for use with the monochrometer could not be made operational

TABLE III

OPTICAL ABSORPTION OF POLYSILICON

Sample ID	thickness microns	R_s ohms	λ = 4500A $\alpha_{poly}t$	λ = 4500A α_{poly} cm^{-1}	λ = 6000A $\alpha_{poly}t$	λ = 6000A α_{poly} cm^{-1}	λ = 7500A $\alpha_{poly}t$	λ = 7500A α_{poly} cm^{-1}
A1	.81	*	3.2	40000	1.1	13000	.32	4000
A2	1.02	*	4.6	46000	1.8	18000	.48	4700
A4	1.48	*	5.3	53000	3.0	20000	.72	4900
A17	.29	2600	1.2	41000	.4	15000	.12	4300
A18	.97	24	4.6	48000	1.8	19000	.46	4700
A19	1.04	1230	4.3	41000	1.6	15000	.46	4400
A21	2.1	9.6	10.9	52000	4.2	20000	.99	4800
A23	2.2	423	11.2	51000	4.2	19000	1.1	4800
A28	.25	187	1.1	44000	.4	14000	.11	4200
A29	.37	98	1.5	41000	.6	16000	.16	4500
A30	.72	59	3.5	49000	1.4	20000	.35	4800
A31	.36	168	1.8	50000	.7	18000	.17	4700
A32	.52	57	3.1	59000	1.2	24000	.27	5100
A33	.61	54	2.5	41000	.9	15000	.26	4200
A34	.54	179	2.6	48000	1.0	19000	.26	4800
A35	.56	92	2.5	45000	.8	15000	.24	4200
A36	.66	52	3.1	47000	1.3	19000	.31	4700
A37	.67	61656	3.3	50000	1.3	20000	.32	4800
A38	.52	96	2.7	51000	1.1	22000	.26	5000
A40	.27	117	1.2	46000	.4	15000	.12	4300

* the sheet resistance was too large to be measured on available instruments

OPTICAL ABSORPTION OF MONOSILICON

wavelength (A)	α_{mono} (cm^{-1})
4500	30000
6000	5000
7500	1700

B) Photovoltaics

Attempts were made to observe photosensitivity in the poly films by pulse illuminating them and monitoring the film resistance. For this purpose, ohmic contact was made to poly films using evaporated aluminum. No such sensitivity was observed.

Poly films were also deposited on tantalum substrates and the current-voltage characteristics of the resultant metal semiconductor junctions were measured. Rectification was observed as shown in Figure 19. A few of these samples also displayed a small degree of light sensitivity.

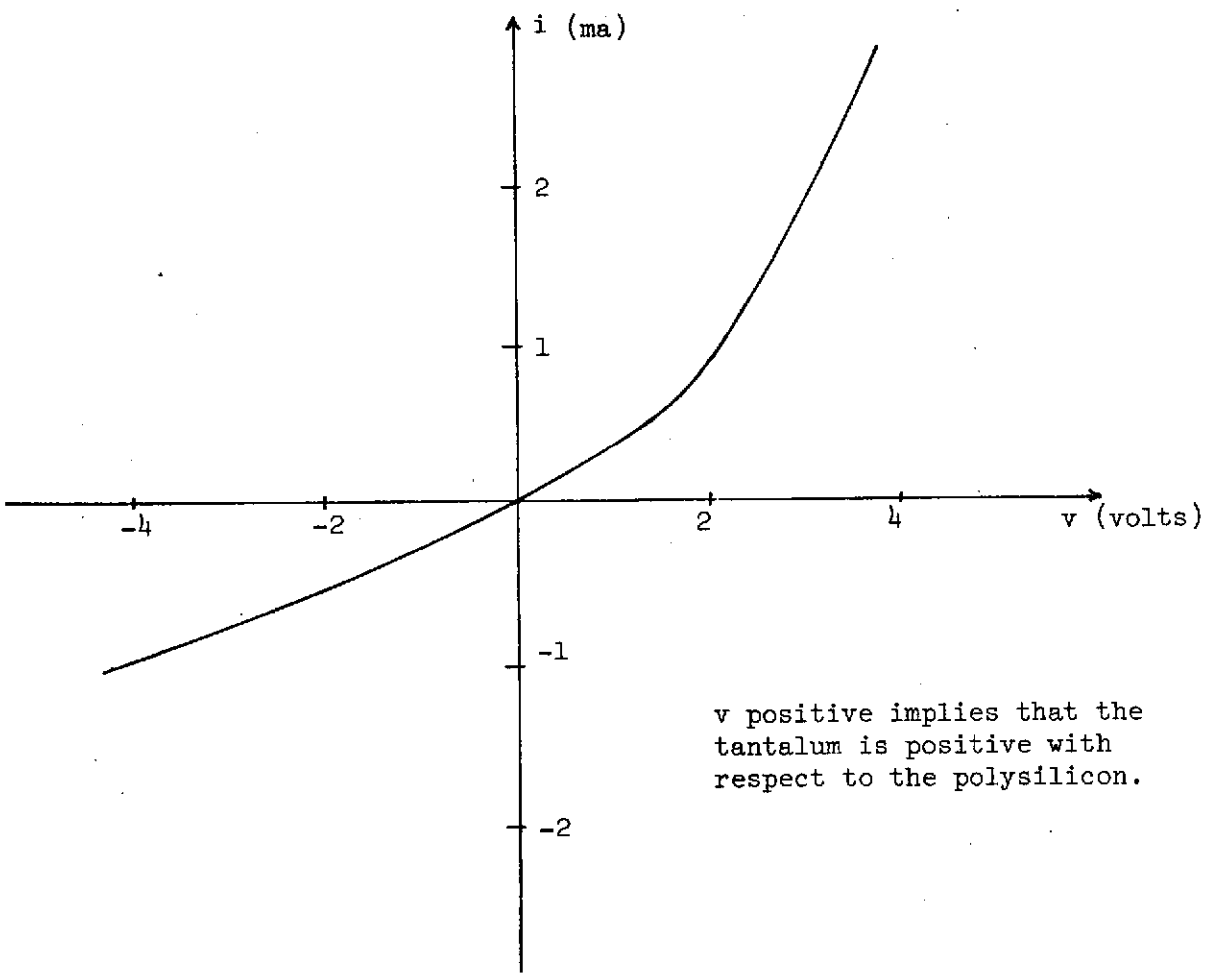

Figure 19

V. CONCLUSIONS

To produce a near transparent electrode for all wavelengths, the final poly thickness should be no greater than 2000 A. A separate diffusion into the poly should be carried out to insure a suitably low sheet resistance. While only p-type diffusions were carried out in this work, n-type diffusions should also prove effective in reducing the sheet resistance.

It is recommended that studies be carried out on poly films of less than 2000 A final thickness since they should display even less absorption than the films grown in this work.

There was no dependence of optical absorption on either the poly growth temperature or the doping gas concentration.

VI. REFERENCES

1. P. E. Gray et al, Physical Electronics and Circuit Models of Transistors, Wiley and Sons, New York, pp32-54 (1964).

2. C. J. Dell'Oca, J. Electrochem. Soc., 119, pp108-111 (1972).

3. T. I. Kamins and C. J. Dell'Oca, J. Electrochem. Soc., 119, pp 112-114 (1972).